Measurement and Correlation of the Thermal Conductivity of Pentafluoroethane (R125) from 190 K to 512 K at Pressures to 70 MPa

Richard A. Perkins* and Marcia L. Huber

Physical and Chemical Properties Division, National Institute of Standards and Technology, Boulder, Colorado 80305-3328

New experimental data on the thermal conductivity of pentafluoroethane (R125) are reported that allow the development of an improved wide-range correlation. These new experimental data, covering a temperature range of 190 K to 390 K and a pressure range of 0.1 to 70 MPa, are used together with available data from the literature to develop a correlation for the thermal conductivity of R125 that covers the temperature range from 190 K to 512 K. The experimental data reported here have an uncertainty of less than 1 % for measurements removed from the critical point and for gas at pressures above 1 MPa, which increases to 3 % in the critical region and for gas at low pressures (<1 MPa). The quality of the primary data sets is such that the thermal conductivity correlation for R125 is estimated to have an uncertainty of about 3 % at a 95 % confidence level, with the exception of state points near the critical point and the dilute gas, where the uncertainty of the correlation increases to 5 %.

Introduction

Accurate thermophysical property data are required for alternative refrigerants such as pentafluoroethane (R125) to allow the design of efficient refrigeration cycles and equipment. Knowledge of the thermal conductivity is necessary to optimally design heat-transfer equipment, such as evaporators and condensers, in refrigeration processes. R125 is used not only as a pure species but also as a component in several refrigerant mixtures that are available commercially. The large uncertainty associated with existing theoretical predictions for the thermal conductivity has motivated efforts to develop empirical correlations to represent the thermal conductivity as a function of temperature and pressure (or density). These correlations are based on accurate experimental data that cover the entire fluid region of interest.

Experimental Section

Two different samples were used in our experiments. The purity of these samples was determined with gas chromatography with a mass spectrometer detector. The sample of R125 that was studied in the subcritical liquid and vapor region contained 0.08 mol % air and 0.0030 mol % water. The sample of R125 that was studied in the supercritical region from 350 K to 390 K contained 0.267 mol % R115, 0.0002 mol % carbon dioxide, and 0.00004 mol % carbon monoxide. The measurements of thermal conductivity were obtained with two transient hot-wire instruments that have previously been described in detail.[1,2] All reported uncertainties are for a coverage factor of $k = 2$, approximately a 95 % confidence interval. Platinum hot wires with a diameter of 12.7 μm functioned as electrical heat sources and as resistance thermometers to measure the temperature rise during the experiment. The outer cavity around the hot wires is copper or stainless steel with a diameter of 9 mm. Each measurement cell consists of a pair of hot wires of differing length operating in a differential arrangement to eliminate errors due to axial conduction. The low-temperature instrument (copper cell) is capable of operation from 30 K to 340 K at pressures to 70 MPa in the liquid, vapor, and supercritical gas phases. The high-temperature instrument (stainless steel cell) is capable of operation from 250 K to 750 K at pressures to 70 MPa in the liquid, vapor, and supercritical gas phases. Initial cell temperatures (T_i) are determined with a reference platinum resistance thermometer with an uncertainty of 0.005 K, and pressures (P_e) are determined with a pressure transducer with an uncertainty of 7 kPa. The basic theory that describes the operation of the transient hot-wire instrument is given by Healy et al.[3] Each hot-wire cell is designed to approximate a transient line source as closely as possible, and deviations from this model are treated as corrections to the experimental temperature rise. The ideal temperature rise (ΔT_{id}) is given by

$$\Delta T_{id} = \frac{q}{4\pi\lambda}\left[\ln(t) + \ln\left(\frac{4a}{r_0^2 C}\right)\right] = \Delta T_w + \sum_{i=1}^{10}\delta T_i \qquad (1)$$

where q is the power applied per unit length, λ is the thermal conductivity of the fluid, t is the elapsed time, $a = \lambda/\rho C_p$ is the thermal diffusivity of the fluid, ρ is the density of the fluid, C_p is the isobaric specific heat capacity of the fluid, r_0 is the radius of the hot wire, $C = 1.781$ ... is the exponential of Euler's constant, ΔT_w is the measured temperature rise of the wire, and δT_i values are corrections[3] to account for deviations from ideal line-source conduction. During analysis, a line is fit to a linear section of the ΔT_{id} versus $\ln(t)$ data, and the thermal conductivity is obtained from the slope of this line. Both thermal conductivity and thermal diffusivity can be determined with the transient hot-wire technique as shown in eq 1, but only the thermal conductivity results are considered here. The experiment temperature (T_e) associated with the thermal conductivity is the average temperature at the wire's surface over the period that was fit to obtain the thermal conductivity. For gas-phase measurements, two corrections[3−7] must be carefully considered. First, since the thermal diffusivity of the gas is much different from that of the wire, the correction for the wire's finite radius becomes very significant. Second, the thermal diffusivity of the dilute gas varies inversely with the pressure, so it is possible for the transient thermal wave to penetrate to the outer boundary

* Corresponding author. E-mail: richard.perkins@nist.gov.

10.1021/je050372t
Published on Web 04/06/2006

of the gas region during an experiment at low pressures.[3−7] The preferred method to deal with such corrections is to minimize them by proper design. For instance, the correction for finite wire radius can be minimized with wires of extremely small diameter (4 to 7) μm, and penetration of the thermal wave to the outer boundary can be eliminated by use of a cell with an outer boundary of large diameter. However, such designs are often not optimal for a general purpose instrument, where such extremely fine wires may be too fragile and large outer dimensions may require too much of a scarce sample, particularly in the liquid phase.

The present transient hot wires require careful correction for the wire's finite radius during such dilute-gas measurements. However, measurement times must be carefully selected to minimize the correction for penetration to the outer boundary due to the relatively small diameter of the concentric fluid region around each hot wire. For the measurements reported here, only application of the full correction[3] for the finite wire dimensions was considered adequate. For a few of the measurements at the lowest pressures, the outer boundary was encountered during the 1-s duration of the experiment, so the experiment time was reduced to minimize the magnitude of this correction. Experiments are generally limited to 1 s in duration, with 250 measurements of temperature rise as a function of elapsed time relative to the onset of wire heating. Fluid convection is normally not a problem, except in the critical region.

R125 is a polar molecule with a significant dipole moment.[8] During measurements on 1,1,1,2-tetrafluoroethane (R134A) with similar bare hot wires, significant electrical conduction and polarization of the fluid during a transient hot-wire measurement was observed.[9] It was further found that less polarization and electrical conduction were observed for very dry samples. Polarization errors were eliminated with a constant-bias voltage applied between the wire and the cell wall.[9] Alternatively, hot wires can be electrically insulated from the fluid during transient hot-wire measurements. However, during the present measurements on R125, neither polarization nor electrical conduction appeared to be significant with bare platinum hot wires. No bias voltage was used during the measurements, and no power dependence was observed in the measured thermal conductivity. Agreement between the present transient hot-wire measurements on R125 and other independent measurements of thermal conductivity will be considered to verify that polarization of the fluid introduced no significant errors.

Experimental Results

The results of measurements of the thermal conductivity of R125 are tabulated in the Supporting Information. The range of state points covered by the present measurements is shown in Figure 1 relative to the vapor-pressure curve of R125 and the primary data sets from the literature that were used to develop the correlation described below. Measurements were reported for four different applied powers at each initial fluid state point to verify the absence of convection during the measurements. There are 162 vapor measurements at temperatures from 300 K to 330 K, 202 liquid measurements at temperatures from 190 K to 330 K, and 633 supercritical measurements at temperatures from 350 K to 390 K reported in the Supporting Information. The liquid and supercritical measurements reach pressures up to 70 MPa. The uncertainty of the measured temperature (ITS-90) is 0.005 K, while the uncertainty of the measured pressure is 7 kPa. The thermal conductivity data have an uncertainty of less than 1 % for measurements removed from the critical point and for gas at pressures above 1 MPa, increasing to 3 % in the critical region and for gas at low pressures (<1 MPa). Reported densities and other fluid property data required for corrections to the measured temperature rise during data analysis are calculated with the equation of state of Lemmon and Jacobsen[10] for each experimental temperature and pressure associated with the measured thermal conductivity.

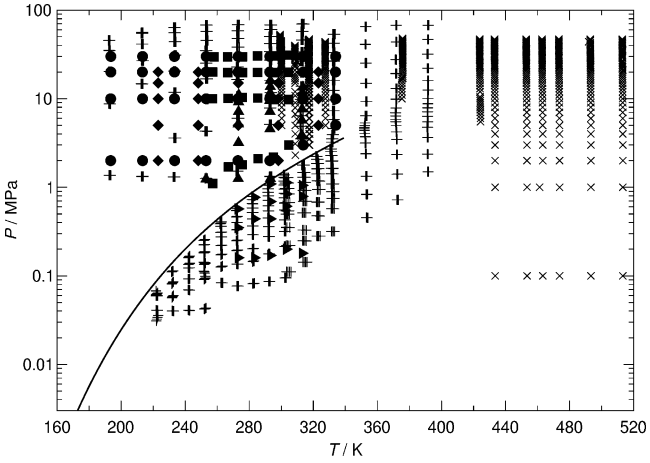

Figure 1. Distribution of the primary data for the thermal conductivity of R125: +, present work; ×, Le Neindre and Garrabos;[30] right-facing solid triangle, Assael et al.;[20] ▲, Assael and Karagiannidis;[21] ●, Gao et al.;[25] ◆, Ro et al.;[28] ■, Yata et al. [38]

Thermal Conductivity Correlation

We represent the thermal conductivity (λ) of a pure fluid as a sum of three contributions:

$$\lambda(\rho, T) = \lambda_0(T) + \Delta\lambda_r(\rho, T) + \Delta\lambda_c(\rho, T) \quad (2)$$

where λ_0 is the dilute-gas thermal conductivity, which depends only on temperature; $\Delta\lambda_r$ is the residual thermal conductivity; and $\Delta\lambda_c$ is the enhancement of the thermal conductivity in the critical region. Both $\Delta\lambda_r$ and $\Delta\lambda_c$ are functions of temperature (T) and density (ρ), with ρ calculated with an equation of state for each given T and P. In this work, we use the equation of state of Lemmon and Jacobsen[10] for R125, which has temperature, pressure, and density limits of 500 K, 60 MPa, and 14.09 mol·L^{-1}. Some of the data in the literature exceed these limits, and the results of these extrapolations should be viewed with caution.

Dilute-Gas Thermal Conductivity. We represent the dilute-gas thermal conductivity as a polynomial in reduced temperature:

$$\lambda_0(T) = \sum_{k=0}^{2} A_k (T/T_c)^k \quad (3)$$

with coefficients A_k, where T is the temperature in K, T_c is the critical temperature in K, and the thermal conductivity is in W·m^{-1}·K^{-1}.

Residual Thermal Conductivity. We used a polynomial in temperature and density to represent the background, or residual, contribution to the thermal conductivity:

$$\Delta\lambda_r(\rho, T) = \sum_{i=1}^{5} \left(B_{i,1} + B_{i,2}\left(\frac{T}{T_c}\right)\right)\left(\frac{\rho}{\rho_c}\right)^i \quad (4)$$

with coefficients $B_{i,j}$, where ρ and ρ_c are the density and critical density in mol·L^{-1}, and the thermal conductivity is in W·m^{-1}·K^{-1}.

Table 1. Summary of Experimental Data and Comparison of the Correlation with Experimental Thermal Conductivity Data for R125[a]

reference	method	uncert/%	purity/%	*T*/K	*P*/MPa	no.of points	AAD	bias	RMS	max. dev.
Asambaev[19] [b]	SSCC	2		170−332	1.16−5.11	12	5.77	−1.86	7.23	−15.44
Assael et al.[20]	**THW**	**1**	**99.95**	**273−313**	**0.16−1.13**	**21**	**1.23**	**−1.18**	**1.15**	**−3.49**
Assael and Karagiannidis[21]	**THW**	**0.5**	**99.95**	**253−313**	**1.24−16.03**	**24**	**1.30**	**−1.30**	**0.89**	**−3.59**
Bivens et al.[22]	THW	1		254−382	0.1, sat.	22	6.28	−4.19	7.51	−18.40
Fellows et al.[23] (also Shankland[24])	THW	1		307−332	sat	6	1.42	−0.06	1.50	−2.04
Gao et al.[25]	**THW**	**0.5**	**99.6**	**193−334**	**2−30**	**32**	**1.17**	**1.11**	**0.83**	**2.40**
Grebenkov et al.[26]	SSCC	3.5	99.9	295−402	2.55−11	74	5.14	5.14	1.58	8.98
Gross and Song[27]	THW	1.6−2	99.8	254−354	0.1−7	102	7.26	−7.20	2.27	−12.82
Ro et al.[28]	**THW**	**2**	**99.8**	**223−323**	**2−20**	**24**	**1.37**	**1.09**	**1.03**	**2.49**
Kraft and Leipertz[29]	DLS	2	99.9	292−338	sat	21	6.86	6.32	5.37	16.37
Le Niendre and Garrabos[30] [b]	**SSCC**	**1.5**	**99.8**	**299−513**	**0.1−53**	**610**	**0.66**	**0.28**	**0.88**	**3.78**
Papadaki and Wakeman[31]	THW	1	99.9	225−306	sat	7	2.36	−2.13	2.06	−6.16
Pitschmann and Straub[32]	DLS, TD	2−5		303−373	1.57−8.76	216	18.18	17.38	24.27	142.1
Pitschmann and Straub[32] [c]	DLS, TP	2−5		303−373	1.57−8.76	197	34.28	29.83	110.3	840.6
Sun et al.[33]	THW	3	99.95	251−334	0.2−2.8	17	3.18	0.90	4.21	12.65
Tanaka et al.[34]	THW	1	99.8	283−333	0.1−2	51	2.57	2.57	1.42	4.95
this work[b]	**THW**	**1−3**		**192−392**	**0.1−70**	**997**	**0.76**	**−0.14**	**0.98**	**−4.07**
Tsvetkov et al.[35]	TCC	2−3	99.83	173−290	sat	16	3.70	−2.32	3.56	−7.70
Tsvetkov et al.[36]	TCC, SSCC	2−3	99.85	187−419	0.1−6	30	3.82	−2.61	3.67	−9.20
Wilson et al.[37]	THW	2	99.7	216−333	0.1-sat	7	5.20	−5.20	2.64	−10.75
Yata et al.[38]	**THW**	**1**	**99.5**	**257−304**	**1.1−30.9**	**24**	**1.54**	**1.27**	**1.44**	**3.56**

[a] THW, transient hot-wire; SSCC, steady-state coaxial cylinder; TCC, transient coaxial cylinder; DLS, derived from dynamic light scattering measurements of thermal diffusivity. TP, based on experimental temperature and pressure; TD, based on experimental temperature and density. Boldface font indicates the data used in the regression. [b] Includes points with temperatures, densities, and/or pressures exceeding the range of validity of the EOS. [c] Excludes critical isochore, based on experimental temperature and pressure.

This form has recently been shown to accurately represent other hydrocarbon fluids such as isobutane,[11] butane,[12] propane,[13] and most recently, dodecane.[14]

Critical Enhancement. Olchowy and Sengers[15] developed a theoretically based, but complex, model for the thermal conductivity enhancement in the critical region. We use a simplified version of their crossover model:[16]

$$\Delta\lambda_c(T, \rho) = \frac{\rho C_p R_0 k_B T}{6\pi\eta\xi}(\Omega - \Omega_0) \tag{5}$$

where the heat capacity at constant pressure, $C_p(T, \rho)$, is obtained from the equation of state; k_B is Boltzman's constant; $R_0 = 1.03$ is a universal constant;[17] and the viscosity, $\eta(T, \rho)$, is obtained from a separate correlation.[18]

The crossover functions Ω and Ω_0 are determined by the following:

$$\Omega = \frac{2}{\pi}\left[\left(\frac{C_p - C_v}{C_p}\right)\arctan(q_d\xi) + \frac{C_v}{C_p}(q_d\xi)\right] \tag{6}$$

$$\Omega_0 = \frac{2}{\pi}\left[1 - \exp\left(\frac{-1}{(q_d\xi)^{-1} + \frac{1}{3}\left(\frac{(q_d\xi)\rho_c}{\rho}\right)^2}\right)\right] \tag{7}$$

The heat capacity at constant volume, $C_v(T, \rho)$, is obtained from the equation of state, and the correlation length (ξ) is given by

$$\xi = \xi_0\left[\frac{P_c\rho}{\Gamma\rho_c^2}\right]^{\nu/\gamma}\left[\left.\frac{\partial\rho(T, \rho)}{\partial P}\right|_T - \frac{T_R}{T}\left.\frac{\partial\rho(T_R, \rho)}{\partial P}\right|_T\right]^{\nu/\gamma} \tag{8}$$

The partial derivative $(\partial\rho/\partial P|_T)$ is evaluated with the equation of state at the system temperature (T) and a reference temperature (T_R). For the reference temperature, we select a value where the critical enhancement is assumed to be negligible: $T_R = 1.5T_c$. The exponents $\gamma = 1.239$ and $\nu = 0.63$ are universal constants.[17] The critical amplitudes Γ and ξ_0 are system-dependent and are determined by the asymptotic behavior of the equation of state in the critical region. The thermal conductivity at the critical point itself is divergent. We have chosen to use values that we consider reasonable[11] for this family of fluids, $\Gamma = 0.0496$ and $\xi_0 = 1.94 \times 10^{-10}$ m. The only parameter left to be determined is the cutoff wavenumber q_d (or alternatively, its inverse q_d^{-1}). When sufficient experimental data are available, q_d is obtained from regression.

Correlation Results

We surveyed the literature for experimental data on R125 and found 18 sources of thermal conductivity data and two sources of thermal diffusivity data, from which thermal conductivity can be derived with the use of an equation of state. Table 1 gives a summary of the experimental data including the type of experimental apparatus, temperature and pressure limits, uncertainty estimates, and sample purity. We identified several data sets (shown in boldface font in Table 1) to be primary data sets. In general, selection as a primary data set involved consideration of sample purity, the authors' estimate of uncertainty (when given), discrepancies with other sets of data, and the experimental procedure used, with preference given to data covering a wide range of conditions. The two most extensive data sets are the present study, comprising 997 points in the liquid, vapor, and supercritical regions at pressures to 70 MPa, and the data of LeNiendre and Garrabos,[30] which contains 610 points obtained with a coaxial cylinder apparatus at temperatures from 300 K to 515 K and at pressures to 53 MPa with an estimated uncertainty of 1.5 %. Two data sets of Assael et al.[20,21] obtained with a transient hot-wire apparatus, and the data of Yata et al.[38] also obtained with a transient hot-wire apparatus cover the temperature range of approximately 253 K to 313 K and were included in the primary data set. Additional data obtained by Gao et al.,[25] and Ro et al.[28] complete the primary data set. Figure 1 shows the distribution of the primary data in terms of pressure and temperature relative to the saturation line.

To obtain the coefficients for the thermal conductivity of the dilute gas in the limit of zero density, eq 3, one can extrapolate the thermal conductivity at constant temperature to zero density,

Table 2. Parameters for the Dilute-Gas Thermal Conductivity (equation 3)

A_0/W·m^{-1}·K^{-1}	$-4.6082 \times 10^{-3} \pm 6.4 \times 10^{-4}$
A_1/W·m^{-1}·K^{-1}	$1.6869 \times 10^{-2} \pm 1.4 \times 10^{-3}$
A_2/W·m^{-1}·K^{-1}	$4.8835 \times 10^{-3} \pm 6.9 \times 10^{-4}$

Table 3: Parameters for the Residual Thermal Conductivity Contribution, Eq. (4−8)

i	j	B_{ij}/W·m^{-1}·K^{-1}
1	1	$-7.2941 \times 10^{-3} \pm 3.5 \times 10^{-3}$
1	2	$1.1050 \times 10^{-2} \pm 3.2 \times 10^{-3}$
2	1	$4.1634 \times 10^{-2} \pm 6.4 \times 10^{-3}$
2	2	$-2.8924 \times 10^{-2} \pm 5.8 \times 10^{-3}$
3	1	$-3.1149 \times 10^{-2} \pm 6.5 \times 10^{-3}$
3	2	$2.7840 \times 10^{-2} \pm 5.2 \times 10^{-3}$
4	1	$1.1268 \times 10^{-2} \pm 2.6 \times 10^{-3}$
4	2	$-1.2110 \times 10^{-2} \pm 2.0 \times 10^{-3}$
5	1	$-1.3832 \times 10^{-3} \pm 3.4 \times 10^{-4}$
5	2	$2.1120 \times 10^{-3} \pm 2.8 \times 10^{-4}$
q_d/m^{-1}		$1.7139 \times 10^{9} \pm 7.4 \times 10^{7}$

provided that there are data over a sufficient range of density along an isotherm. An alternative method is to simultaneously fit the dilute-gas thermal conductivity, the excess contribution, and the critical enhancement (eqs 2 to 8), in order to obtain the dilute-gas coefficients A_i, the excess coefficients B_{ij}, and the cutoff wavenumber q_d. We chose the latter method, with equilibrium properties from the equation of state of Lemmon and Jacobsen[10] and the critical point $T_c = 339.17$ K, $P_c = 3.6177$ MPa, and $\rho_c = 4.779$ mol/L. We used the fitting program ODRPACK[39] to fit the primary experimental data, with equal weights of one, to determine the coefficients in eqs 2 to 8, given in Tables 2 and 3. Table 1 gives the average absolute deviation, bias, root-mean-square, and maximum deviations of the correlation from the experimental data. In the tables, we use the following definitions: average absolute deviation, AAD = $100/n(\Sigma|(\lambda_i^{calc}/\lambda_i^{exp} - 1)|)$; bias = $100/n(\Sigma(\lambda_i^{calc}/\lambda_i^{exp} - 1))$, and root-mean-square deviation RMS^2 = $100/n(\Sigma(\lambda_i^{calc}/\lambda_i^{exp} - 1)^2)$ − bias^2, where each summation ranges from $i = 1$ to n and n is the number of data points. The state conditions of some of the data points exceeded the limits of the EOS; their results are still included in the statistical analysis, but we recommend caution when extrapolating outside the limits of the EOS.

Primary Data Results. There are generally two or more primary data sets available over most of the temperature and pressure range for temperatures below 390 K as shown in Figure 1. The primary data set of LeNeindre and Garrabos[30] is the only one available at temperatures above 390 K for R125. Figure 2 shows deviations between the primary data along specific isotherms from 298 K to 314 K where they overlap. In the vapor phase, the present results are about 1.5 % higher than the data of Assael et al.[20] (1 % uncertainty). In the liquid phase, the present results fall between the data of Assael and Karagiannidis[21] (0.5 % uncertainty) and the data sets of LeNeindre and Garrabos[30] (1.5 % uncertainty) and Gao et al.[25] (0.5 % uncertainty). These four primary data sets agree with each other within their uncertainties. The data set of Ro et al.[28] (2 % uncertainty) is 3 % lower than the present results, while the data set of Yata et al.[38] (1 % uncertainty) is 4 % lower than the present results. The data set of Yata et al.[38] agrees only with the primary data set of Ro et al.[28] within its claimed uncertainty, while the data set of Ro et al.[28] agrees with most of the other primary data sets within its uncertainty.

It is noteworthy that the data of LeNeindre and Garrabos,[30] obtained with the steady-state concentric-cylinder technique, are in excellent agreement with the other primary data sets obtained with the transient hot-wire technique. This good agreement

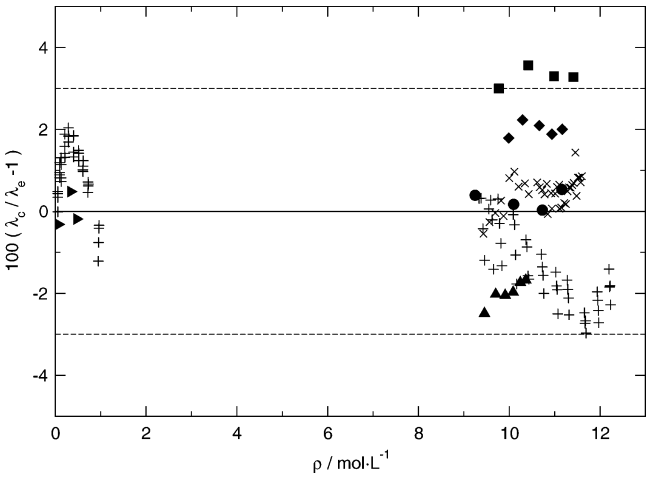

Figure 2. Relative deviations between the primary data at temperatures from 298 K to 314 K and the present correlation for R125 as a function of the calculated density:[10] +, present work (313 K); ×, Le Neindre and Garrabos[30] (309 K); right-facing solid triangle, Assael et al.[20] (313 K); ▲, Assael and Karagiannidis[21] (313 K); ●, Gao et al.[25] (314 K); ◆, Ro et al.[28] (298 K); ■, Yata et al.[38] (304 K).

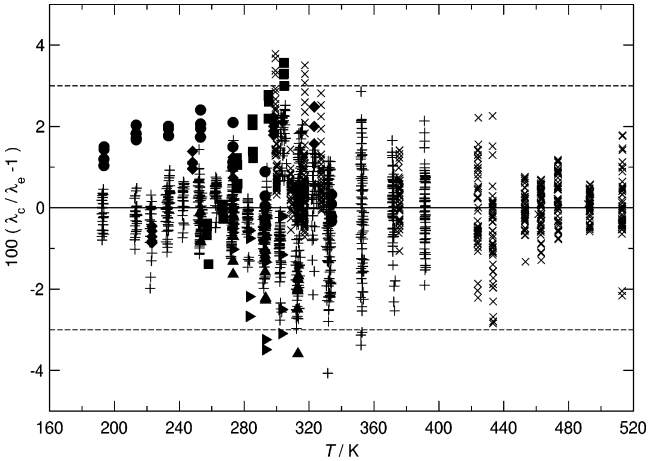

Figure 3. Relative deviations between the primary data and the present correlation for R125 as a function of temperature from 190 K to 512 K: +, present work; ×, Le Neindre and Garrabos;[30] right-facing solid triangle, Assael et al.;[20] ▲, Assael and Karagiannidis;[21] ●, Gao et al.;[25] ◆, Ro et al.;[28] ■, Yata et al.[38]

supports our observation that polarization of our sample of R125 did not introduce significant errors, even though bare hot wires were used for the present transient hot-wire measurements of thermal conducivity. Figure 3 shows deviations between the primary data and the correlation as a function of measured temperature. Figure 4 shows deviations between the primary data and the correlation as a function of density calculated from the measured temperature and pressure with the equation of state of Lemmon and Jacobsen.[10] The correlation accurately represents the primary data over the temperature range from 190 K to 520 K for the liquid, vapor, and supercritical fluid phases at pressures up to 70 MPa. All of the primary data sets agree with the correlation to within ± 3 % at a 95 % confidence level. It is expected that the correlation has significantly larger uncertainties at temperatures and densities that are closer to the critical point than the primary data.

Secondary Data Deviations. The temperature and pressure distribution of the secondary data sets relative to the saturation line is shown in Figure 5. The secondary data sets that were not fit during the correlation development have larger uncertainties than the primary data sets that were fit to develop the

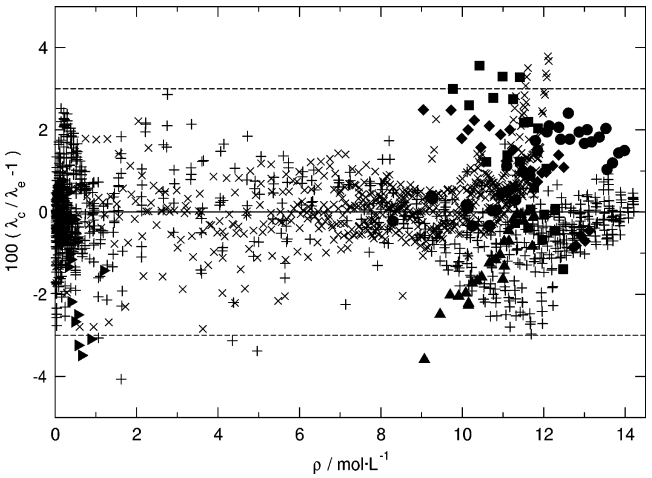

Figure 4. Relative deviations between the primary data and the present correlation for R125 as a function of the calculated density:[10] +, present work; ×, Le Neindre and Garrabos;[30] right-facing solid triangle, Assael et al.;[20] ▲, Assael and Karagiannidis;[21] ●, Gao et al.;[25] ◆, Ro et al.;[28] ■, Yata et al. [38]

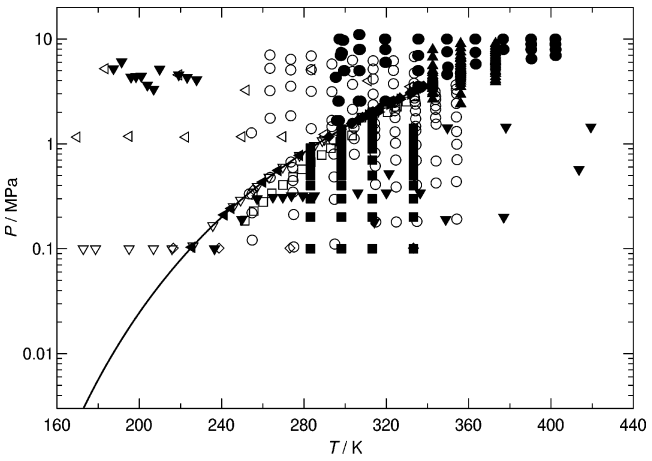

Figure 5. Distribution of the secondary data for the thermal conductivity of R125: ◇, Wilson et al.;[37] left-facing solid triangle, Papadaki and Wakeham;[31] ■, Tanaka et al.;[34] right-facing solid triangle, Fellows et al.;[23] left-facing open triangle, Asambaev;[19] ▼, Tsvetkov et al.;[36] ▽, Tsvetkov et al.;[35] □, Sun et al.;[33] ○, Gross and Song;[27] right-facing open triangle, Bivens et al.;[22] ●, Grebenkov et al.;[26] ◆, Kraft and Leipertz[29]; ▲, Pitschmann and Straub[32] (*T*, *P*); △, Pitschmann and Straub[32] (*T*, *ρ*).

correlation. The secondary data sets have an upper pressure limit of only 10 MPa as compared to 70 MPa for the primary data. Figure 6 shows the relative deviations between the secondary data and the present correlation in terms of temperature, while Figure 7 shows these deviations in terms of density. The largest deviations between the secondary data and the correlation are in the critical region. Relative deviations between the secondary data and the correlation range from −18 % to 24 %.

The secondary data sets of Asambaev[19] and Tsvetkov et al.[35] provide liquid data at temperatures lower than the primary data sets, covering the region from 170 K to 190 K. These two data sets generally agree with the correlation to within 5 %, except for the lowest temperature data point of Asambaev,[19] which is 14 % higher and appears to be an outlier. There is a general trend in these data sets of increasing deviations as temperature is decreased below 200 K. The correlation shows reasonable extrapolation for liquids to temperatures below the 190 K limit of the primary data in Figure 6. These two data sets were not included in the primary data, since they have different temperature dependence and values seem to be lower than the primary data sets at temperatures near 300 K.

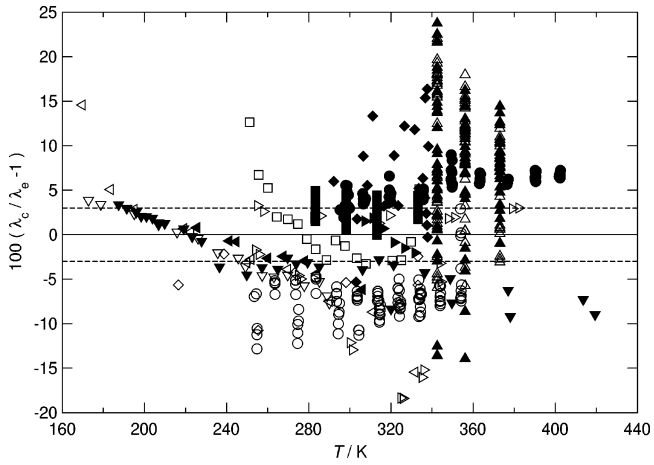

Figure 6. Relative deviations between the secondary data and the present correlation for R125 over the temperature range from 160 K to 440 K: ◇, Wilson et al.;[37] left-facing solid triangle, Papadaki and Wakeham;[31] ■, Tanaka et al.;[34] right-facing solid triangle, Fellows et al.;[23] left-facing open triangle, Asambaev;[19] ▼, Tsvetkov et al.;[36] ▽, Tsvetkov et al.;[35] □, Sun et al.;[33] ○, Gross and Song;[27] right-facing open triangle, Bivens et al.;[22] ●, Grebenkov et al.;[26] ◆, Kraft and Leipertz[29]; ▲, Pitschmann and Straub[32] (*T*, *P*); △, Pitschmann and Straub[32] (*T*, *ρ*).

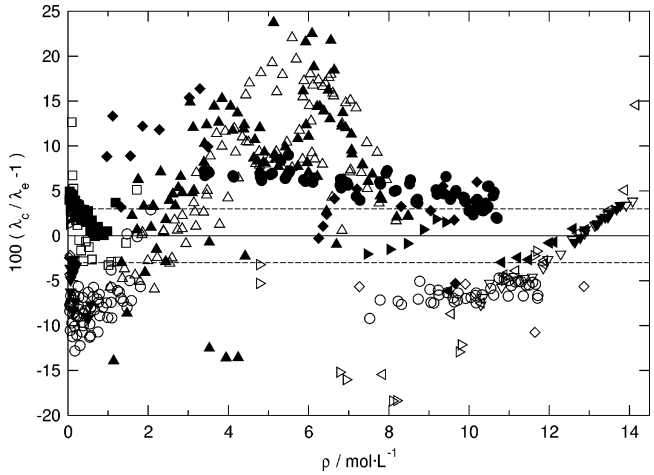

Figure 7. Relative deviations between the secondary data and the present correlation for R125 as a function of the calculated density:[10] ◇, Wilson et al.;[37] left-facing solid triangle, Papadaki and Wakeham;[31] ■, Tanaka et al.;[34] right-facing solid triangle, Fellows et al.;[23] left-facing open triangle, Asambaev;[19] ▼, Tsvetkov et al.;[36] ▽, Tsvetkov et al.;[35] □, Sun et al.;[33] ○, Gross and Song;[27] right-facing open triangle, Bivens et al.;[22] ●, Grebenkov et al.;[26] ◆, Kraft and Leipertz[29]; ▲, Pitschmann and Straub[32] (*T*, *P*); △, Pitschmann and Straub[32] (*T*, *ρ*).

Kraft and Leipertz[29] and Pitschmann and Straub[32] reported thermal diffusivity data obtained from dynamic light scattering (DLS). These dynamic light scattering measurements do not require a macroscopic temperature gradient and approach the critical point very closely. However, an accurate equation of state is required to convert the measured thermal diffusivity to thermal conductivity. The equation of state must be accurate at the temperatures and pressures studied. Because the fluid is very compressible in the critical region, extremely small errors in measured pressure translate to large errors in calculated density. Pitschmann and Straub[32] report measured temperature, pressure (uncertainty of 0.01 MPa), and density (uncertainty of 1.8 %) obtained from measurements of refractive index. Thus, deviations shown for the Pitschmann and Straub[32] data are considered here based on the measured temperature and pressure (TP) and the measured temperature and density (TD). Many of these DLS measurements were simply too close to the critical point for

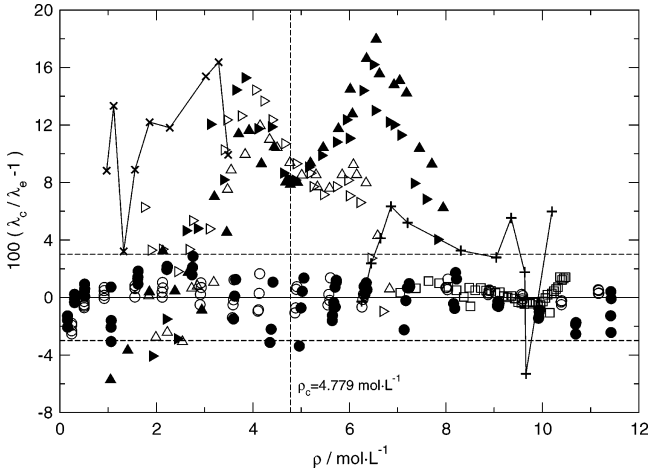

Figure 8. Relative deviations between selected data within ± 35 K of the critical temperature (339.17 K) and the present correlation for R125 as a function of the calculated density:[10] ●, present results (353 K); ○, present results (372 K); □, Le Neindre and Garrabos[30] (375 K); ▲, Pitschmann and Straub[32] ($T \approx 356$ K, ρ); right-facing solid triangle, Pitschmann and Straub[32] ($T \approx 356$ K, P); △, Pitschmann and Straub[32] ($T \approx 373$ K, ρ); right-facing open triangle, Pitschmann and Straub[32] ($T \approx 373$ K, P); +, Kraft and Leipertz[29] (saturated liquid); ×, Kraft and Leipertz[29] (saturated vapor).

the reference equation of state[10] to give reliable results, so they were not considered here. The TP results should be better for data removed from the critical region, since the equation of state has much less uncertainty in density than the density from refractive index measurement. The TD results should be better in the critical region where the uncertainty in the pressure measurement translates to larger density uncertainties. The data of Kraft and Leipertz[29] were measured for saturated R125, so densities were calculated from the measured temperature. The deviations of the light-scattering data are best seen in Figure 7 as a function of density. The largest deviations shown are up to 24 % near the critical density of 4.779 mol·L^{-1} for the Pitschmann and Straub[32] data. Figure 6 shows that the deviations between the saturation measurements of Kraft and Leipertz[29] and the correlation increase to 16 % as the temperature increases up to the critical temperature of 339.17 K.

These large deviations in the DLS data sets are attributed to large uncertainties in the density and specific heat used to convert thermal diffusivity to thermal conductivity in the critical region. There is also a secondary impact from the equation of state, since increased uncertainty in the properties needed for the correlation in eqs 5 to 8 results in increased uncertainty in the correlation itself very close to the critical point. Figure 8 shows deviations of selected supercritical isotherms from transient hot wires (present results), concentric cylinders,[30] and dynamic light scattering[32] near 353 K and 373 K. There is good agreement between transient hot-wire measurements and steady-state concentric cylinder measurements of thermal conductivity at 373 K but systematic disagreement with the DLS measurements of thermal diffusivity.[32] The deviations between the DLS data at 373 K and the present correlation exhibit a maximum that it not centered at the critical density as would be expected if the cutoff wavenumber (q_d) was simply in error. Figure 8 also shows the DLS data of Kraft and Leipertz[29] for saturated liquid and vapor at temperatures from 300 K to the critical temperature. It is seen that there is large scatter in the DLS data[29] for the saturated vapor phase relative to the correlation. There is less scatter in the DLS data[29] for the saturated liquid phase near the critical point, and the DLS data agree with the present correlation within 6 %. Additional work is needed, possibly with a crossover model or scaled equation of state, before a thermal conductivity correlation can be developed for R125 that is accurate very close to the critical point.

Outside of the critical region, the secondary data generally agree with the present correlation to within ± 10 %. The thermal conductivity values of Gross and Song[27] and Bivens et al.[22] are generally higher that the primary data sets and the correlation, as are the data sets of Asambaev[19] and Tsvetkov et al.[35] at temperatures in the vicinity of 300 K. The data set of Grebenkov et al.[26] is generally lower than the primary data sets and the correlation. The lowest temperature values of Sun et al.[33] are lower than the primary data, with a different temperature behavior. Good agreement, within ± 5 %, is found with most of the other secondary data sets.

Conclusions

A total of 997 measurements of the thermal conductivity of R125 are reported for the liquid, vapor, and supercritical fluid phases over the temperature range from 190 K to 390 K with pressures up to 70 MPa. The thermal conductivity data for R125 have an uncertainty of less than 1 % for measurements removed from the critical point and for gas at pressures above 1 MPa, increasing to 3 % in the critical region and for gas at low pressures (<1 MPa) at a 95 % confidence level. A significant critical enhancement is observed in the thermal conductivity data near the critical point. A correlation for the thermal conductivity of R125 is developed based on these measurements and six other reliable data sets from the literature. The correlation requires thermodyamic property information that is obtained from the equation of state of Lemmon and Jacobsen.[10] This correlation accounts for the critical enhancement with a crossover model and agrees with the primary data sets to within ± 3 % at a 95 % confidence level over the temperature range from 190 K to 512 K. The correlation is expected to have increased uncertainty in the region near the critical point and at temperatures and pressures beyond the range of the underlying equation of state. Comparison with literature data at temperatures below 190 K indicates reasonable extrapolation to temperatures between 170 K and 190 K with an increased uncertainty of 5 % for thermal conductivity.

Acknowledgment

The authors acknowledge the work of John B. Howley, who made some of the thermal conductivity measurements reported here. The authors appreciate valuable discussions with Prof. Carlos Nieto de Castro regarding polarization of refrigerant samples during transient hot-wire measurements.

Supporting Information Available:

Tabulated experimental values are reported. This material is available free of charge via the Internet at http://pubs.acs.org.

Literature Cited

(1) Perkins, R. A.; Roder, H. M.; Nieto de Castro, C. A. A high-temperature transient hot-wire thermal conductivity apparatus for fluids. *J. Res. Natl. Inst. Stand. Technol.* **1991**, *96*, 247−269.

(2) Roder, H. M. A transient hot wire thermal conductivity apparatus for fluids. *J. Res. Natl. Bur. Stand.* **1981**, *86*, 457−493.

(3) Healy, J.; DeGroot, J. J.; Kestin, J. The theory of the transient hot-wire method for measuring the thermal conductivity. *Physica* **1976**, *C82*, 392−408.

(4) Assael, M. J.; Karagiannidis, L.; Richardson, S. M.; Wakeham, W. A. Compression work using the transient hot-wire method. *Int. J. Thermophys.* **1992**, *13*, 223−235.

(5) Taxis, B.; Stephan, K. The measurement of the thermal conductivity of gases at low density by the transient hot-wire technique. *High Temp.−High Pressures* **1994**, *15*, 141−153.

(6) Li, S. F. Y.; Papadaki, M.; Wakeham, W. A. The measurement of the thermal conductivity of gases at low density by the transient hot-wire technique. *High Temp.−High Pressures* **1993**, *25*, 451−458.
(7) Li, S. F. Y.; Papadaki, M.; Wakeham, W. A. Thermal conductivity of low-density polyatomic gases. In *Thermal Conductivity 22*; Tong, T. W., Ed.; Technomic Publishing: Lancaster, PA, 1994; pp 531−542.
(8) Cabral, B. J. C.; Guedes, R. C.; Pai-Panandiker, R. S.; Nieto de Castro, C. A. Hydrogen bonding and internal rotation of hydrofluorocarbons by density functional theory. *Phys. Chem. Chem. Phys.* **2001**, *3* (19), 4200−4207.
(9) Perkins, R. A.; Laesecke, A.; Nieto de Castro, C. A. Polarized transient hot wire thermal conductivity measurements. *Fluid Phase Equilib.* **1992**, *80*, 275−286.
(10) Lemmon, E. W.; Jacobsen, R. T. A new functional form and new fitting techniques for equations of state with application to pentafluoroethane (HFC-125). *J. Phys. Chem. Ref. Data* **2005**, *34*, 69−108.
(11) Perkins, R. A. Measurement and correlation of the thermal conductivity of isobutane from 114 K to 600 K at pressures to 70 MPa. *J. Phys. Chem. Ref. Data* **2002**, *47* (5), 1272−1279.
(12) Perkins, R. A.; Ramires, M. L. V.; de Castro, C. A. N.; Cusco, L. Measurement and correlation of the thermal conductivity of butane from 135 K to 600 K at pressures to 70 MPa. *J. Chem. Eng. Data* **2002**, *47* (5), 1263−1271.
(13) Marsh, K. N.; Perkins, R. A.; Ramires, M. L. V. Measurement and correlation of the thermal conductivity of propane from 86 to 600 K at pressures to 70 MPa. *J. Chem. Eng. Data* **2002**, *47* (4), 932−940.
(14) Huber, M. L.; Laesecke, A.; Perkins, R. A. Transport properties of *n*-dodecane. *Energy Fuels* **2004**, *18*, 968−975.
(15) Olchowy, G. A.; Sengers, J. V. Crossover from regular to singular behavior of the transport properties of fluids in the critical region. *Phys. Rev. Lett.* **1988**, *61*, 15−18.
(16) Olchowy, G. A.; Sengers, J. V. A simplified representation for the thermal conductivity of fluids in the critical region. *Int. J. Thermophys.* **1989**, *10* (2), 417−426.
(17) Krauss, R.; Weiss, V. C.; Edison, T. A.; Sengers, J. V.; Stephan, K. Transport properties of 1,1-difluoroethane (R152a). *Int. J. Thermophys.* **1996**, *17* (4), 731−757.
(18) Huber, M. L.; Laesecke, A. Correlation for the viscosity of pentafluoroethane (R125) from the triple point to 500 K at pressures up to 60 MPa. *Ind. Eng. Chem. Res.* In press.
(19) Asambaev, A. Z. Thermal conductivity of liquid and gaseous freons and their mixtures. Ph.D. Thesis, St. Petersburg, USSR, 1992.
(20) Assael, M. J.; Malamataris, N.; Karagiannidis, L. Measurements of the thermal conductivity of refrigerants in the vapor phase. *Int. J. Thermophys.* **1997**, *18* (2), 341−352.
(21) Assael, M. J.; Karagiannidis, L. Measurements of the thermal-conductivity of liquid R32, R124, R125, and R141b. *Int. J. Thermophys.* **1995**, *16* (4), 851−865.
(22) Bivens, D. B.; Yokozeki, A.; Geller, V. Z.; Paulaitis, M. E. In *Transport Properties and Heat Transfer of Alternatives for R502 and R22*; ASHRAE/NIST Refrigerants Conference, Gaithersburg, MD, August 19−20, 1993; ASHRAE: Gaithersburg, MD, 1993; pp 73−84.
(23) Fellows, B. R.; Richard, R. G.; Shankland, I. R. In *Thermal Conductivity Data for Some Environmentally Acceptable Fluorocarbons*; Cremers, C. J., Fine, H. A., Eds.; Thermal Conductivity 21; Plenum Press: New York, 1990; pp 311−325.
(24) Shankland, I. R. Transport properties of CFC alternatives. Presented at the AIChE Spring National Meeting, Orlando, FL, 1990.
(25) Gao, X.; Yamada, T.; Nagasaka, Y.; Nagashima, A. The thermal conductivity of CFC alternatives HFC-125 and HCFC-141b in the liquid phase. *Int. J. Thermophys.* **1996**, *17* (2), 279−292.
(26) Grebenkov, A. J.; Kotelevsky, Y. G.; Saplitza, V. V.; Beljaeva, O. V.; Zajatz, T. A.; Timofeev, B. D. In *Experimental Study of Thermal Conductivity of Some Ozone Safe Refrigerants and Speed of Sound in their Liquid Phase, CFCs: The Day After*; Joint Meeting of IIR Commissions B1, B2, E1, and E2, Padova, Italy, September 21−23, 1994; IIR: Padova, Italy, 1994; pp 419−429.
(27) Gross, U.; Song, Y. W. Thermal conductivities of new refrigerants R125 and R32 measured by the transient hot-wire method. *Int. J. Thermophys.* **1996**, *17* (3), 607−619.
(28) Ro, S. T.; Kim, M. S.; Jeong, S. U. Liquid thermal conductivity of binary mixtures of difluoromethane (R32) and pentafluoroethane (R125). *Int. J. Thermophys.* **1997**, *18* (4), 991−999.
(29) Kraft, K.; Leipertz, A. Thermal diffusivity and ultrasonic velocity of saturated R125. *Int. J. Thermophys.* **1994**, *15* (3), 387−399.
(30) Le Neindre, B.; Garrabos, Y. Measurements of the thermal conductivity of HFC-125 in the temperature range from 300 to 515 K and at pressures up to 53 MPa. *Int. J. Thermophys.* **1999**, *20* (5), 375−399.
(31) Papadaki, M.; Wakeham, W. A. Thermal-conductivity of R32 and R125 in the liquid-phase at the saturation vapor-pressure. *Int. J. Thermophys.* **1993**, *14* (6), 1215−1220.
(32) Pitschmann, M.; Straub, J. The thermal diffusivity of refrigerants R32, R125, and R143a. *Int. J. Thermophys.* **2002**, *23* (4), 877−904.
(33) Sun, L.-Q.; Zhu, M.-S.; Han, L.-Z.; Lin, Z.-Z. Thermal conductivity of gaseous difluoromethane and pentafluoroethane near the saturation line. *J. Chem. Eng. Data* **1997**, *42* (1), 179−182.
(34) Tanaka, Y.; Matsuo, S.; Taya, S. Gaseous thermal conductivity of difluoromethane (HFC-32), pentafluoroethane (HFC-125), and their mixtures. *Int. J. Thermophys.* **1995**, *16* (1), 121−131.
(35) Tsvetkov, O. B.; Laptev, Y. A.; Asambaev, A. G. Thermal conductivity of refrigerants R123, R134a, and R125 at low-temperatures. *Int. J. Thermophys.* **1994**, *15* (2), 203−214.
(36) Tsvetkov, O. B.; Kletski, A. V.; Laptev, Y. A.; Asambaev, A. J.; Zausaev, I. A. Thermal conductivity and PVT measurements of pentafluorethane (refrigerant HFC-125). *Int. J. Thermophys.* **1995**, *16* (5), 1185−1192.
(37) Wilson, L. C.; Wilding, W. V.; Wilson, G. M.; Rowley, R. L.; Felix, V. M.; Chisolm-Carter, T. Thermophysical properties of HFC-125. *Fluid Phase Equilib.* **1992**, *80*, 167−177.
(38) Yata, J.; Hori, M.; Kobayashi, K.; Minamiyama, T. Thermal conductivity of alternative refrigerants in the liquid phase. *Int. J. Thermophys.* **1996**, *17* (3), 561−571.
(39) Boggs, P. T.; Byrd, R. H.; Rogers, J. E.; Schnabel, R. B. *ODRPACK, Software for Orthogonal Distance Regression*; NISTIR 4834; National Institute of Standards and Technology: Gaithersburg, MD, 1992.

Received for review September 12, 2005. Accepted March 4, 2006. The authors acknowledge support of the Building Equipment Division, Office of Building Technologies, U.S. Department of Energy, under Grant DE-FG02-91CE23810.

JE050372T